ACS OMEGA

Open Access

http://pubs.acs.org/journal/acsodf

Article

Reviving the Potential of Vermiculite-Based Adsorbents: Exceptional Ibuprofen Removal on Novel Amide-Containing Gemini Surfactants

Xianqi Hu* and Zhuang Ma

Cite This: *ACS Omega* 2024, 9, 4841−4848

Read Online

ACCESS | Metrics & More | Article Recommendations | Supporting Information

ABSTRACT: In this study, we introduce a novel series of gemini surfactants with amide groups (HDAB, HDAHD, and HDAPX) and use these surfactants to decorate sodium vermiculite (Na-Vt) for the adsorption of Ibuprofen (IBP) from wastewater. Exceptional IBP uptake on organo-vermiculites (organo-Vts) is obtained, with maximum adsorption capacities reaching 249.87, 342.21, and 460.15 mg/g for HDAB-Vt, HDAHD-Vt, and HDAPX-Vt (C_0 = 500 mg/L, modifier dosage = 0.2 CEC), respectively. The adsorption of IBP is well fitted by pseudo-second-order, intraparticle diffusion, and Freundlich isotherm models, verifying chemical adsorption processes with multilayer arrangement of IBP in organo-Vts. Thermodynamically, the removal of IBP on HDAHD-Vt is exothermic, while the endothermic nature aptly describes the adsorption process of HDAB-Vt and HDAPX-Vt. Moreover, organo-Vts can be stably regenerated in three cycles. Outstanding adsorption performance of organo-Vts is attributed to synergistic effects of the partition process and functional interaction, which are influenced by the steric hindrance and chain configuration of the modifier. A combined evaluation of adsorption tests and fitting calculations is employed to reveal the adsorption mechanism: (i) the incorporation of amides into the alkyl chain significantly enhances the utilization of the interlayer space in organo-Vts. (ii) Smaller steric hindrance and higher rigidity of the modifier spacer contribute to improved adsorption performance. The findings in this study rekindle interest in Vt-based adsorbents, which demonstrate comparable potential to other emerging adsorbents that are yet to be fully explored.

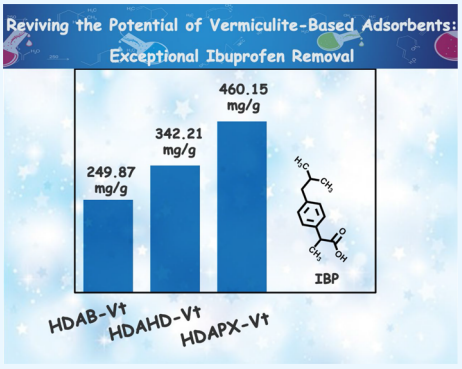

1. INTRODUCTION

Gemini surfactants (geminis) consist of two amphiphilic chains linked by a spacer, owning particular performances compared to their monomeric counterparts. These distinctive properties have opened up a wide range of industrial applications in enhanced oil recovery, material synthesis, and adsorption technology.[1] Benefited from their straightforward synthesis routes and structural stability, geminis with alkyl quaternary ammonium have been extensively explored for the design of hybrid materials. These materials can be tailored to meet specific requirements for pollutant adsorption.[2−4] In light of growing environmental concerns, the introduction of amide groups into geminis offers several advantages, which not only enhances biodegradability but also augments their surface/interface activity.[5]

The intercalation of gemini surfactants into clay minerals, named as organic modification, represents a popular strategy for expanding the interlayer environment, enhancing hydrophobic nature, and introducing functional groups into hybrid materials.[4] The modifier availability and clay property are crucial factors affecting the adsorptivity of organoclays. These properties are closely associated with the characteristics of the clay mineral and the organic modifier. (i) Concerning the clay minerals, the charge property significantly influences the loading amount of modifier molecules. In this regard, clays with higher layer charges, like vermiculite (Vt), have demonstrated superior performance compared to montmorillonite and silica nanosheets.[6,7] (ii) Regarding the structure of the modifier, the characteristics of the alkyl chain and spacer play a pivotal role in shaping both the morphology and the structural stability of organo-vermiculites (organo-Vts).[8−10] The spacer group within modifier molecules can vary in terms of polarity, flexibility, length, and rigidity, and these attributes would further influence the adsorptivity and mechanism of the resulting organo-Vts.

Rigid functional group (such as unsaturated bond or aromatic ring) within the surfactant act as effective adsorption sites for organic pollutant, where the instability of unsaturated bonds limits the in-depth investigation and adsorption cycle of the corresponding organo-Vt adsorbents.[5] Aromatic rings, characterized by their high π-electron density, have been proven to improve the structural stability of organoclays. Rigid

Received: October 24, 2023
Revised: December 22, 2023
Accepted: December 25, 2023
Published: January 18, 2024

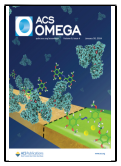

https://doi.org/10.1021/acsomega.3c08363
ACS Omega 2024, 9, 4841−4848

spacers tend to enlarge the interlayer of organoclays more effectively, but excessive rigid functional groups can create severe steric hindrance, weakening the effectiveness in adsorptivity.[11] Derived from the obvious aggregation effect, modifiers containing aromatic groups are more efficient at expanding the interlayer space.[12] Biphenyl gemini surfactants (BHBP) with higher π-electron density have been shown to exhibit stronger $\pi-\pi$ interactions compared to dipyridyl-containing gemini surfactants (DHBP).[8] Despite the synergistic effects of hydrophobicity and $\pi-\pi$ interactions contributing to the arrangement of modifiers, the specific influence of the modifier spacer, location, and number of functional groups on the interlayer environment and adsorptivity of organo-vermiculites remains relatively unclear.

Ibuprofen (IBP) is a widely utilized nonsteroidal anti-inflammatory drug (NSAID), whose presence in wastewater and surface water systems has raised potential environmental concerns.[13,14] Research has investigated the adsorption of IBP on vermiculite-based adsorbents modified with quaternary alkylammonium salts in their bromide form. The maximum adsorption capacities of Vt-EHDDMA and Vt-HDTMA for IBP were 52 ± 2 and 54 ± 2 mg/g, respectively.[15] However, these capacities are lower compared to other IBP adsorbents with quinoline-containing organo-vermiculites (240.69 mg/g).[16] Presently, most research has centered on the development of organo-vermiculites by optimizing alkyl chain length and spacer structures, whereas limited attention was devoted to the incorporation of functional groups into the alkyl chain. These functional groups are pivotal in mediating interactions between IBP and modifiers, presenting an opportunity to further enhance the adsorption efficiency.

The overarching objective of this study is to formulate a series of gemini surfactants (HDAB, HDAHD, and HDAPX) to explore the adsorption performance of organo-vermiculites (organo-Vts). These organo-Vts are anticipated to exhibit exceptional adsorption performance toward IBP. The structural characteristics of the resulting organo-Vts are systematically examined by using various characterization methods. Comprehensive analyses of the adsorption kinetics, isotherms, and thermodynamics are examined. The adsorption processes are elucidated by scrutinizing influential factors and fitting experimental data. Remarkably, the developed organo-Vts display remarkable recyclability, enabling a thorough assessment of regeneration and reusability. Significantly, a novel "functional connector" concept is validated, involving the incorporation of functional groups into the alkyl chain of the modifier. This concept proves effective in enhancing the adsorptivity of organo-Vts by simultaneously incorporating specific functional groups into the alkyl chain and spacer of gemini surfactants.

2. EXPERIMENTS

2.1. Materials. Vermiculite (Vt) was obtained from Shanghai Aladdin Biochemical Technology Co., Ltd., and underwent pretreatment with sodium carbonate (Na_2CO_3), sourced from Macklin. The resulting Na-vermiculite (Na-Vt) exhibited a cationic exchange capacity (CEC) of 126 mmol/100 g.[17] The source materials for the synthesis of modifiers, including *N*,*N*-dimethyl-1,3-propylene amide (NDPE), palmitic acid, 1,4-dibromobutane, hydrochloric acid, n-propanol, epichlorohydrin, and dibromo-*p*-xylene, were obtained from Macklin. Reaction catalysts such as phosphorus acid and NaOH, as well as IBP, the solvent ethyl acetate, and isopropanol were procured from Macklin.

2.2. Synthesis of Gemini Surfactants. A two-step route was applied for synthesizing the target gemini surfactants.[18] The initial step involved the preparation of hexadecamide propyl dimethylamide, following a procedure outlined in a relevant literature source.[18] Here is a brief description of the synthesis process: in a 100 mL three-necked flask, NDPE (35 mmol) was mixed with palmitic acid (100 mmol, 26.03 g) under oxygen-free conditions. Subsequently, the catalyst phosphorus acid was gradually added (0.4 wt % of the total mass). Intermediate product with yellow oily state was obtained after refluxing at 120 °C for 8 h (labeled as PKO-16).

In the second step, PKO-16 (26.59 g) was mixed with 10 mmol of 1,4-dibromobutane (or the spacer 1,3-dibromonpropanol, synthesized according to a related literature study[19] or p-diromobenzyl) in 100 mL of isopropanol. A catalyst, NaOH (0.1 g), was added. After reacting at 80 °C for 24 h, white powder as the crude produce was received. The final product was obtained through washing with ethyl acetate and standing at room temperature for 24 h. The final products were designated as 1,3−2(hexadecamide propyl dimethylammonium chloride) *n*-butane (HDAB), 1,3−2(hexadecamide propyl dimethylammonium chloride)-2-hydroxypropane dichloride (HDAHD), and 1,3−2(hexadecamide propyl dimethylammonium chloride)-*p*-xylene (HDAPX). The synthetic routes of these surfactants are depicted in Figure 1. The purities of HDAB, HDAHD, and HDAPX are assessed through elemental analysis (EA) and Fourier transform infrared spectroscopy (FT-IR).

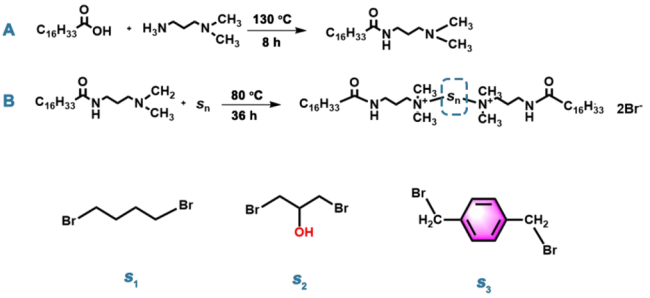

Figure 1. Two-step synthetic routes (step A: the synthesis of the intermediate product; step B: the synthesis of the final product) of HDAB (s1), HDAHD (s2), and HDAPX (s3).

2.3. Adsorption Test. Standard adsorption experiments were conducted to evaluate the adsorption mechanism of organo-vermiculites (organo-Vts). A comprehensive analysis of various influencing factors, such as modifier dosage, adsorption time, initial IBP concentration, temperature, and solution pH, was carried out. The adsorption mechanism, which encompasses aspects such as adsorption kinetics, isotherms, and thermodynamics, was systematically investigated. In these experiments, 0.03 g of organo-Vts were mixed with 30 mL of IBP solution under varying conditions.[20,21] The concentration of IBP was quantified by using UV−vis spectroscopy. Detailed calculations related to adsorption capacity and mechanisms can be found in the Supporting Information.

3. RESULTS AND DISCUSSION

3.1. Characterization. *3.1.1. FT-IR Spectra of Modifier and Organo-Vts.* The FT-IR spectra of HDAB, HDAHD, and

https://doi.org/10.1021/acsomega.3c08363
ACS Omega 2024, 9, 4841−4848

HDAPX are presented in Figure 2. Broad peaks at 3345 cm^{-1} correspond to the vibrations of −OH in physically adsorbed water molecules.[22] The stretching vibrations of −C−H (resulting from $-CH_2$ and $-CH_3$) are evident at 2940 and 2813 cm^{-1}, with their bending vibration occurring at 1439 cm^{-1}. Peaks associated with benzene are observable in the 1500−1600 cm^{-1} range, partially overlapping with the C═O peak at 1641 cm^{-1} and the C−N peak at 1528 cm^{-1}. Furthermore, the vibration of N−H is observed at 701 cm^{-1}.[23] EA data are listed in Table S1. Consulting the results from FT-IR and EA, it can be inferred that the synthesized modifiers are the intended target products with high purity.

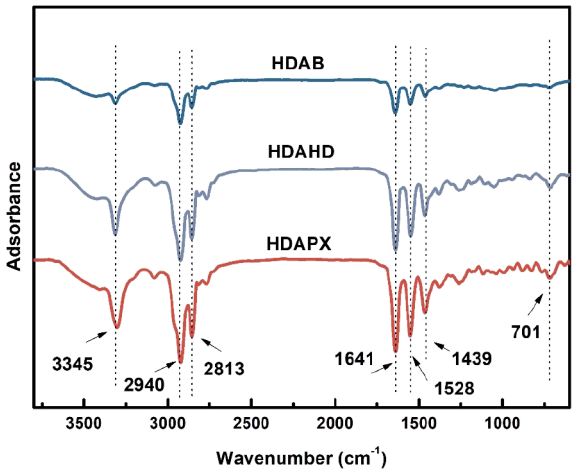

Figure 2. FT-IR spectra of HDAB, HDAHD, and HDAPX.

As shown in Figure 3a, Na-Vt is proved hydrophilic, with the prominent peaks at 3435 and 1627 cm^{-1} in the corresponding FT-IR spectrum,[24] corresponding to −OH groups. The peak at 998 cm^{-1} is due to the Si−O vibration. Emergence of peaks at 2917/2844 and 1461 cm^{-1} proves the presence of modifiers in organo-Vts. Comparing these modifier-related peaks to the $-CH_2$ vibrations observed in Figure 2 (at 2945/2848 and 1461 cm^{-1}), a slight shift of these peaks is indicative of changes in the $-CH_2$ configuration. This shift can be attributed to the confinement effect of the interlayer space on the modifier molecules.[25] The discrepancies in the FT-IR spectra between Na-Vt and organo-Vts clearly indicate the successful intercalation or adsorption of surfactant molecules into Na-Vt.

3.1.2. XRD Analysis of Organo-Vts. The XRD patterns of organo-Vts are shown in Figure 3b−d. It is possible to deduce the arrangement of the modifiers based on the modifier structure and interlayer environment of organo-Vts.[26] In the context of modifier arrangement, a larger interlayer spacing results in a relative loose stacking of modifiers within organo-Vts.

In comparison to the d_{001} spacing of Na-Vt (1.46 nm), organo-Vts show obviously enlarged interlayer spacings, even at low modifier dosages (specifically 5.16, 4.93, and 4.80 nm for HDAB-Vt, HDAHD-Vt, and HDAPX-Vt at 0.2−0.4 CEC).

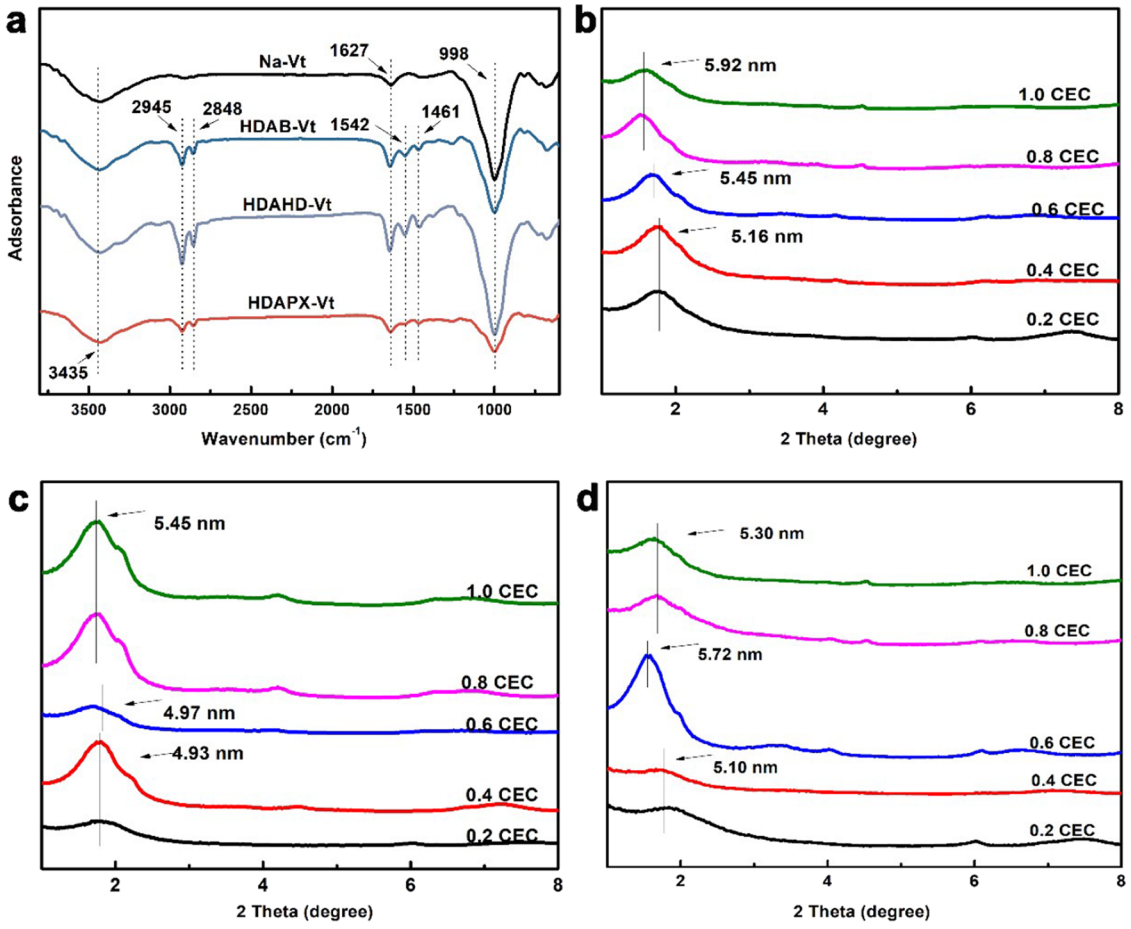

Figure 3. FT-IR spectra (a) and XRD patterns of HDAB-Vt (b), HDAHD-Vt (c), and HDAPX-Vt (d).

https://doi.org/10.1021/acsomega.3c08363
ACS Omega 2024, 9, 4841−4848

The calculation of the interlayer distance involves minus the layer thickness of Na-Vt (0.96 nm) from the d_{001} value of organo-Vts.[8] Consequently, the corresponding interlayer distances for HDAB-Vt, HDAHD-Vt, and HDAPX-Vt at 0.2 CEC are 4.20, 3.97, and 3.84 nm, respectively, representing a typical paraffin-bilayer arrangement. The relatively narrower interlayer spacing of HDAPX-Vt at low modifier dosages may be attributed to the aggregation of modifiers resulting from stronger intermolecular interactions between HDAPX molecules.

When the modifier amount gradually increases to 0.6 CEC, the d_{001} spacing also increases (from 5.16/4.93/4.80 to 5.45/4.97/5.72 nm), indicating an increment in the contact angles between the modifier chain and the plane of Na-Vt. Under modifier dosages of 0.8−1.0 CEC, the d_{001} spacings of HDAB-Vt, HDAHD-Vt, and HDAPX-Vt reach 5.92, 5.45, and 5.30 nm, respectively.

3.1.3. TG-DTG Analysis of Organo-Vts. The decomposition of physically adsorbed water molecules in Na-Vt and organo-Vts (as depicted in Figures S1 and 4) is associated with the

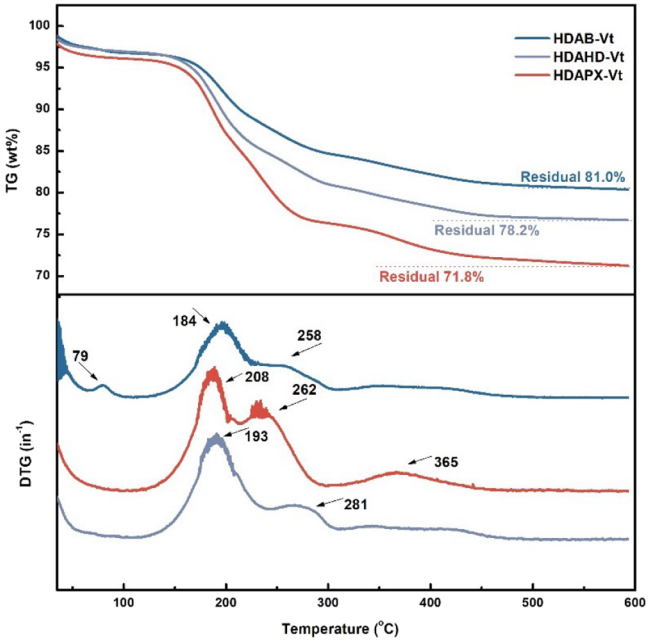

Figure 4. TG-DTG curves of HDAB-Vt, HDAHD-Vt, and HDAPX-Vt.

obvious weight loss temperatures below 100 °C. It is worth noting that the hydrophobic organo-Vts contain significantly fewer water molecules.[27] Additional weight losses occurring between 200 and 400 °C in organo-Vts are attributed to the decomposition of adsorbed/intercalated modifiers. Specifically, HDAB-Vt, HDAHD-Vt, and HDAPX-Vt show distinct weight losses at 184, 193/281, and 208/262 °C, respectively.[28] Consulting to the modifier structure, interactions between modifiers and Na-Vt mainly involve electrostatic interaction (derived from the headgroup of modifier and Na-Vt), van der Waals force (derived from the alkyl chain between modifiers), hydrogen bonds (resulted from the amide group and hydroxyl group in the modifier), and $\pi-\pi$ interactions (derived from the aromatic-containing spacer in the modifier),[23] which are closely related to specific decomposition temperatures in DTG curves. Based on results from TG-DTG, these interactions vary in strength, with the ranking as follows: VDW force < hydrogen bond < $\pi-\pi$ interaction < electrostatic interaction.[29] Modifiers exhibit a preference for bonding with Na-Vt through physical adsorption, as evidenced by their greater weight losses at low-temperature stages compared with Na-Vt. The pronounced role of the $\pi-\pi$ interaction is supported by the relatively lowest decomposition temperature in HDAPX-Vt. In the TG curves of organo-Vts, the total weight losses for HDAB-Vt, HDAHD-Vt, and HDAPX-Vt (occurring above 100 °C) are approximately 17.6, 18.5, and 18.9 wt %, respectively. These values exhibit a similar trend with EA results, with deviations within 1.5 wt %, aligning with the total element contents (Table 1).

Table 1. Elemental Analysis Results (wt %) of Na-Vt and Organo-Vts

sample	C	H	N
Na-Vt	0.41	0.82	0.13
HDAB-Vt	18.03	3.58	2.72
HDAHD-Vt	18.24	3.92	2.88
HDAPX-Vt	13.65	2.36	1.74

Conclusions can be drawn from the above results: (i) the modifier loading on per weight of Na-Vt is 0.36 mmol for HDAB, 0.34 mmol for HDAHD, and 0.28 mmol for HDAPX. (ii) The modifier availability, defined as the ratio of the modifier loaded to the added amount, is 72.1% for HDAB-Vt, 68.5% for HDAHD-Vt, and 50.5% for HDAPX-Vt.

3.2. Adsorption Experiment. *3.2.1. Effect of Modifier Dosage on IBP Adsorption.* By applying the single modifier and/or Na-Vt for IBP adsorption, the function of organic modification is revealed: (i) modifiers are soluble in a water environment and cannot adsorb IBP. (ii) The hydrophilic nature of Na-Vt results in negligible IBP removal. Therefore, organic modification is essential for both surfactants and Na-Vt. Following modification, organo-Vts exhibit a remarkable increased adsorption capacity, as depicted in Figure 5, with the IBP adsorption amounts reaching 322.6, 404.7, and 489.9 mg/g (C_0 = 500 mg/L, T = 25 °C), correspond to different optimal modifier dosages of organo-Vts (HDAB-Vt (0.4 CEC), HDAHD-Vt (1.0 CEC), and HDAPX-Vt (1.0 CEC),

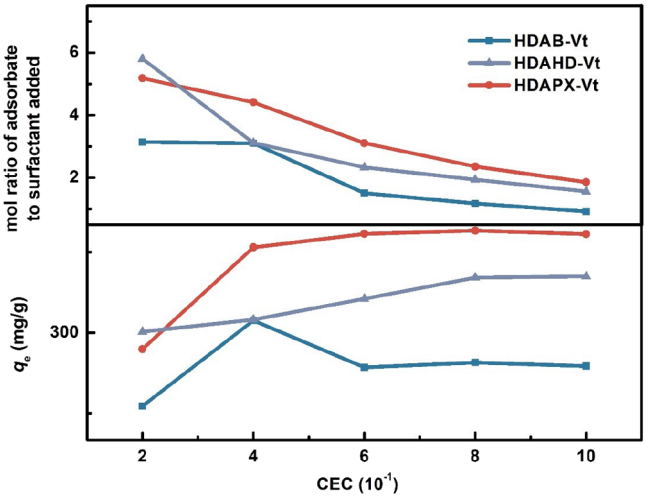

Figure 5. Effect of modifier dosage and mole ratio of IBP to surfactant added.

https://doi.org/10.1021/acsomega.3c08363
ACS Omega 2024, 9, 4841−4848

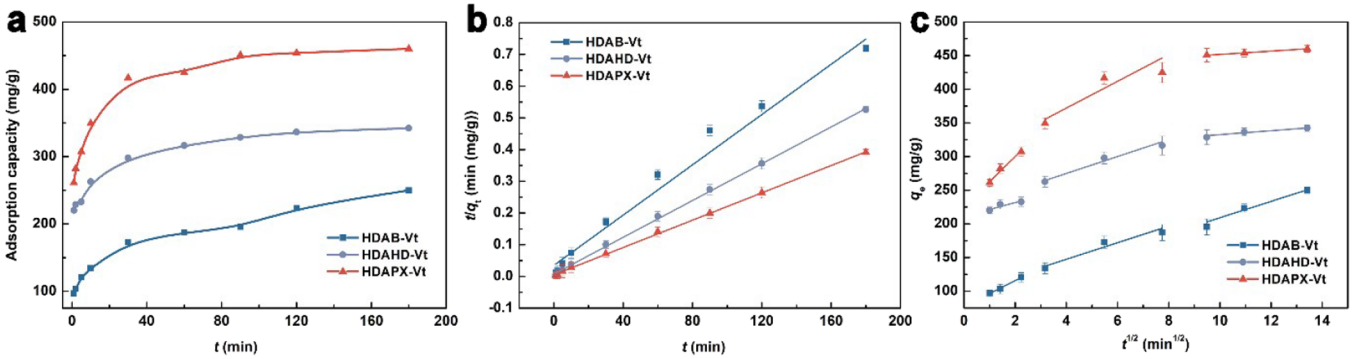

Figure 6. Effect of time on IBP adsorption (a), PSO kinetic model (b), and IPD model (c).

Table 2. Kinetic Parameters for the Adsorption of IBP on Organo-Vts[a]

		pseudo-first-order				pseudo-second-order					intraparticle diffusion			
adsorbent	$q_{e,exp}$	$q_{e,cal}$	k_1 (10^{-2})	R^2	SSE	$q_{e,cal}$	k_2 (10^{-4})	k_2q_e	R^2	SSE (10^{-3})	k_{id}	C (10^2)	R^2	SSE (10^2)
HDAB-Vt	249.87	225.88	3.1	0.7481	8.68	245.10	4.61	0.11	0.9800	9.46	11.52	1.02	0.8738	0.94
HDAHD-Vt	342.21	121.51	2.6	0.9869	0.26	343.64	10.60	0.36	0.9992	0.19	11.75	2.28	0.9399	0.45
HDAPX-Vt	460.15	167.34	2.9	0.9800	0.48	462.96	8.26	0.38	0.9994	0.07	16.52	3.07	0.6657	5.75

[a] $q_{e,exp}$ (mg g^{-1}), $q_{e,cal}$ (mg g^{-1}), k_1 (min^{-1}), k_2 (g mg^{-1} min^{-1}), k_{id} (mg g^{-1} $min^{1/2}$), C (mg g^{-1}).

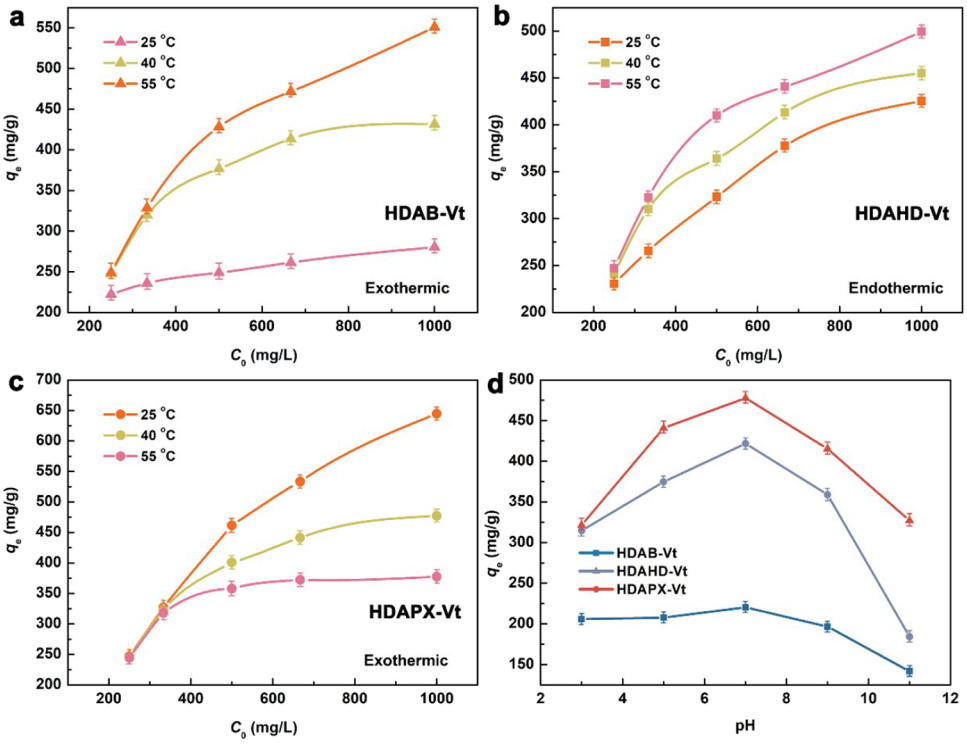

Figure 7. Effects of concentration/temperature on IBP adsorption on the HDAB-Vt (a), HDAHD-Vt (b), and HDAPX-Vt (c) and the effect of pH on IBP adsorption (d).

respectively). The corresponding removal efficiencies are 64.52, 80.94, and 97.98% for HDAB-Vt, HDAHD-Vt, and HDAPX-Vt, respectively.

When IBP is adsorbed onto traditional organo-Vts, the role of the spacer acts as a functional site, while the alkyl chain serves as a partitioning medium.[10] The important impact of chain amides on the adsorption capacity of organo-Vts is evident in two ways: (i) enlargement of the interlayer space of organo-Vts, allowing for the accommodation of more IBP molecules. (ii) Functioning as a "functional connector" to provide adsorptive sites and enhance the interaction between surfactants and IBP molecules.

The adsorption capacities of organo-Vts increase as the modifier dosage is raised from 0.2 to 0.4 CEC. A continuous increase in modifier dosage contributes to an obvious increment in the adsorption capacity of HDAPX-Vt, nearing adsorption equilibrium for HDAB-Vt, but causes a diminishing effect on HDAB-Vt. Within the range of lower modifier dosages (0.2−0.4 CEC), HDAB-Vt, HDAHD-Vt, and HDAPX-Vt show similar adsorption trends, validating that

https://doi.org/10.1021/acsomega.3c08363
ACS Omega 2024, 9, 4841−4848

Table 3. Adsorption Isotherm Constants for Adsorption of IBP on Organo-Vts

adsorbent	temperature	Langmuir			Freundlich		
		q_{max}	K_L	R^2	K_f	n	R^2
HDAB-Vt	298 K	265.09	0.16	0.5949	172.72	14.22	0.9356
	313 K	403.46	0.52	0.8256	236.54	10.25	0.9735
	328 K	478.23	0.83	0.7198	258.43	8.31	0.9835
HDAHD-Vt	298 K	453.48	0.33	0.8452	172.72	14.22	0.9426
	313 K	425.32	0.13	0.8726	236.54	10.25	0.9842
	328 K	397.34	0.05	0.7032	258.43	8.31	0.9934
HDAPX-Vt	298 K	374.29	0.33	0.9868	235.91	10.68	0.8934
	313 K	450.92	0.24	0.9745	223.75	6.08	0.9530
	328 K	583.69	0.20	0.9102	225.54	4.26	0.9813

Table 4. Thermodynamic Parameters for IBP on Organo-Vts

adsorbent	$\Delta G°$(kJ/mol)			$\Delta S°$(kJ/(mol K))	$\Delta H°$(kJ/mol)
	T = 298 K	T = 313 K	T = 328 K		
HDAB-Vt	2.18	2.91	4.87	−16.38	48.74
HDAHD-Vt	−3.75	−2.56	−3.73	7.07	−24.76
HDAPX-Vt	2.28	3.63	6.78	−1.48	42.06

the alkyl chain plays a pivotal role in IBP adsorption, while the effect of the spacers is of secondary importance. Excessive modifiers, on the other hand, result in severe steric hindrance, which is more pronounced for HDAB due to its more flexible structure. For a comprehensive assessment of organo-Vts, we selected 0.6 CEC as the optimal modifier dosage for subsequent adsorption experiments.

3.2.2. Effect of Time and Adsorption Kinetics. As shown in Figure 6a,b, HDAHD-Vt and HDAPX-Vt display similar adsorption trends, reaching equilibrium at approximately 120 min. In contrast, the adsorption of IBP on HDAB-Vt exhibits a slower adsorption rate, requiring 180 min to reach equilibrium. The maximum experimental adsorption capacities of HDAB-Vt, HDAHD-Vt, and HDAPX-Vt are 249.87, 342.21, and 460.15 mg/g under the conditions of C_0 = 500 mg/L, T = 25 °C, modifier dosage = 0.6 CEC and t = 180 min, respectively. We applied the pseudo-first-order (PFO), pseudo-second-order (PSO), and intraparticle diffusion (IPD) models (as presented in Table 2) to analyze the adsorption mechanism.[30] Kinetics provides insight into the speed with which IBP molecules are taken up by organo-Vts. This includes identifying the stages of adsorption, assessing the rate-limiting steps, and obtaining information about how quickly equilibrium is reached. When compared with the PFO model, the PSO model appears to be more suitable for describing the equilibrium data. This conclusion is supported by higher R^2 values, lower sum of squared errors (SSE) values, and a better consistency between $q_{e,cal}$ and $q_{e,exp}$. These findings suggest that IBP adsorption is primarily a chemically controlled process.[31]

The involvement of intraparticle diffusion process is evident from the clear delineation of the IPD model into three distinct stages (Figure 6c), relevant to external diffusion, intraparticle diffusion, and equilibrium.[32] We can draw several conclusions from the IPD model analysis (as summarized in Table 2): (i) the relatively high R^2 values in the second stage (Table 2) underscore the significant role of the intraparticle diffusion process, demonstrating the critical importance of the interlayer environment of organo-Vts for IBP adsorption. (ii) In the course of IBP adsorption, a higher value of k_{id} indicates a faster diffusion rate, which can be ranked as follows: HDAPX-Vt > HDAHD-Vt > HDAB-Vt. This ranking suggests that a rigid spacer (aromatic-containing group), which can provide strong $\pi-\pi$ binding sites for IBP, is more conducive to a faster diffusion process. Conversely, spacers with greater steric hindrance result in slower diffusion rates. (iii) The trends in the thickness of the boundary layer (C) are consistent with the adsorptivity trend of organo-Vts. Greater value of C of HDAPX-Vt is due to the stronger $\pi-\pi$ stacking interactions between the adsorbed IBP molecules and those dissolved in solution.[33] Notably, the smallest value of C indicates the weakest $\pi-\pi$ stacking effect in HDAB-Vt.

3.2.3. Effect of IBP Concentration and Adsorption Isotherm. It is evident that the adsorption capacity increases as the IBP concentration rises (Figure 7a−c). The adsorption capacities for HDAB-Vt, HDAHD-Vt, and HDAPX-Vt are 550.82, 499.23, and 644.63 mg/g, respectively (at a temperature of 25 °C and an initial concentration of C_0 = 1000 mg/L). The highest IBP uptake on HDAPX-Vt can be attributed to two key factors: (i) $\pi-\pi$ interactions between HDAPX and IBP molecules and (ii) a suitable interlayer environment for accommodating IBP molecules.

Compared to the Langmuir model (as shown in Table 3), it is evident that the Freundlich isotherm model is more agreeable for the adsorption processes of HDAB-Vt, HDAHD-Vt, and HDAPX-Vt. This suggests that IBP molecules tend to bond to the heterogeneous adsorption sites in a multilayer arrangement.[34] Moreover, higher temperatures promote molecular motion and chain flexibility, facilitating the bilayer arrangement of the IBP molecules.

3.2.4. Effect of Temperature and Adsorption Thermodynamics. We have observed varying adsorption capacities with changes in the temperature for different organo-Vts. Specifically, HDAHD-Vt shows a decrease in the adsorption capacity with increasing temperature, while HDAB-Vt and HDAPX-Vt exhibit the opposite trend in their adsorption behavior. To better understand these observations, we have calculated the thermodynamic parameters, which are presented in Table 4 (C_0 = 1000 mg/L). For HDAHD-Vt, the negative standard enthalpy $\Delta H°$ (−24.76 kJ/mol) indicates an exothermic adsorption process.[35] Furthermore, negative $\Delta G°$ and positive $\Delta S°$ values suggest that the process is spontaneous and associated with a decrease in randomness.[36] On the other

https://doi.org/10.1021/acsomega.3c08363
ACS Omega 2024, 9, 4841−4848

hand, HDAB-Vt and HDAPX-Vt display an endothermic nature, accompanied by nonspontaneous property and increased randomness during the whole adsorption process.[37]

These differences in thermodynamic behavior between HDAHD-Vt and HDAB/HDAPX-Vts can be attributed to variations in the steric hindrance of the chain and spacer in the modifier structure. It is commonly observed that interactions between IBP and surfactants are exothermic.[35] In a flexible chain environment, the diffusion of IBP, as well as the interactions between IBP and surfactant molecules, is more preferred.

3.2.5. Effect of pH. To further investigate the stability and reliability of organo-Vts, we examined the adsorption behavior in relation to the solution pH (as depicted in Figure 7d). The variation in IBP adsorption can be attributed to a synergistic effect between IBP dissociation (with a pK_a of 4.45) and the surface charge of the adsorbent.

Organo-Vts display similar adsorption trends with changing solution pH: there is a gradual increase in IBP uptake within the pH range of 3−7, followed by a sharp decline under alkaline conditions, ultimately resulting in the lowest IBP uptake at a pH of 11.[38] The relatively high IBP uptake at lower pH values can be attributed to electrostatic interactions between IBP and the negatively charged surface of organo-Vts. However, when the pH is between 9 and 11, the negative charge on the surface of the IBP molecule gradually increases, leading to electrostatic repulsion, which in turn reduces the adsorption capacities of organo-Vts. In terms of adsorption capacities under the same solution pH, organo-Vts can be ranked as follows: HDAB-Vt > HDAHD-Vt > HDAPX-Vt.

In summary, interactions between organo-Vts and IBP include partition process (derived from the alkyl chain in the modifier), hydrogen bonds (derived from the amide group in the modifier), electrostatic interaction (derived from the surface charge of organo-Vts), and $\pi-\pi$ interaction (derived from the aromatic ring in the modifier). After the adsorption of IBP molecules in organo-Vts, the existence of a benzene ring in the IBP structure may act as additive interaction sites for adsorption of the IBP molecules in solution, forming $\pi-\pi$ stacking interactions between different IBP molecules.

3.3. Regeneration. In light of cost and environmental considerations, reproducibility is gaining widespread recognition. After ethanol pickling, organo-Vts can be regenerated with a slight reduction in adsorptivity. This suggests the emergence of new adsorption sites even if some are partially lost. HDAB-Vt and HDAHD-Vt can be reused for up to three cycles, accompanied by fluctuating adsorptivity from 249.87 to 185.72 mg/g and from 342.21 to 298.65 mg/g, respectively. Differences in adsorption capacity between consecutive cycles are primarily attributed to additional and persistent interactions between organo-Vts and IBP. However, the adsorption capacities of HDAPX-Vt toward IBP noticeably decrease after three cycles, dropping from 460.15 to 205.38 mg/g. This decrease may be attributed to the irreversible adjustment of IBP molecules to the chain configuration, resulting in a structural change in the corresponding organo-Vts. Desorption tests effectively support an economically and sustainably viable adsorption−desorption cycle for organo-Vts, especially in the case of HDAHD-Vt, which offers suitable adsorption capacity and the most stable regenerability.

4. CONCLUSIONS

In this study, effective removal of IBP is achieved by modifying Na-vermiculite (Na-Vt) with a series of novel amide-based gemini surfactants (HDAB, HDAHD, and HDAPX). Through FT-IR, XRD, and TG-DTG analysis, we have confirmed enhanced hydrophobicity, an expanded interlayer environment, and increased organic carbon content in the resulting organo-vermiculites (organo-Vts). These modifications are influenced by the spacer rigidity and steric hindrance of the surfactant molecules. Exceptional adsorption of IBP on organo-Vts has been achieved, with maximum IBP adsorption capacities reaching 249.87, 342.21, and 460.15 mg/g on HDAB-Vt, HDAHD-Vt, and HDAPX-Vt, respectively. PSO and IPD models are suitable to describe the adsorption processes, and the majority of them are in accordance with Freundlich isotherms. Thermodynamically, the removal of IBP on HDAHD-Vt is exothermic, while endothermic nature aptly describes the adsorption process of HDAB-Vt and HDAPX-Vt. The excellent adsorption performance of organo-Vts is attributed to the synergistic effect of the hydrophobic interaction, hydrogen bonds, electrostatic interaction, $\pi-\pi$ interaction, and $\pi-\pi$ stacking. The adsorptivity of organo-Vts is further influenced by the steric hindrance and chain configuration of surfactants. A comprehensive analysis of adsorption tests, theoretical simulations, and characterizations has yielded insights into the adsorption mechanism: (i) the amides in the alkyl chain, serving as "functional connector" sites for IBP, significantly enhance the utilization of the interlayer space in organo-Vts. (ii) The smaller steric hindrance and stronger rigidity of the modifier spacer result in improved uptake toward target organic pollutants. In conclusion, the practical applications of this study can be expected not only in terms of "resource cleaner" and "energy cleaner" but also introduce organo-Vts with comprehensive capabilities of excellent adsorption, stable regeneration, and easy separation. These properties not only support a sustainable adsorption cycle but also effectively avoid the generation of hazardous byproducts.

■ ASSOCIATED CONTENT

Supporting Information

The Supporting Information is available free of charge at https://pubs.acs.org/doi/10.1021/acsomega.3c08363.

Experimental details of characterization, adsorption experiment, adsorption kinetics, isotherms, and thermodynamics; elemental analysis data of HDAB, HDAHD, and HDAPX; and TG curve of Na-Vt (PDF)

■ AUTHOR INFORMATION

Corresponding Author

Xianqi Hu − *Department of Chemical Engineering, Hebei Petroleum University of Technology, Hebei 067000, P. R. China*; Email: huxianqi@cdpc.edu.cn

Author

Zhuang Ma − *Department of Chemical Engineering, Hebei Petroleum University of Technology, Hebei 067000, P. R. China*; orcid.org/0009-0007-6038-9619

Complete contact information is available at: https://pubs.acs.org/10.1021/acsomega.3c08363

https://doi.org/10.1021/acsomega.3c08363
ACS Omega 2024, 9, 4841−4848

Notes

The authors declare no competing financial interest.

REFERENCES

(1) Shen, T.; Gao, M. Gemini surfactant modified organo-clays for removal of organic pollutants from water: A review. *Chem. Eng. J.* **2019**, *375*, No. 121910.

(2) Akram, M.; et al. An Insight View on Synthetic Protocol, Surface Activity, and Biological Aspects of Novel Biocompatible Quaternary Ammonium Cationic Gemini Surfactants. *J. Surfactants Deterg.* **2021**, *24* (1), 35−49.

(3) Guo, N.; Zheng, M.; Wang, X. Research progress on synthesis and application of anionic-cationic Gemini surfactants. *Petrochem. Technol.* **2019**, *48* (4), 419−425.

(4) Awad, A. M.; et al. Adsorption of organic pollutants by natural and modified clays: A comprehensive review. *Sep. Purif. Technol.* **2019**, *228*, No. 115719.

(5) Yang, W.; et al. Amide Gemini surfactants linked by rigid spacer group 1,4-dibromo-2-butene: Surface properties, aggregate and application properties. *J. Mol. Liq.* **2021**, *326*, No. 115339.

(6) Ding, F.; et al. Comparative study of organo-vermiculite, organo-montmorillonite and organo-silica nanosheets functionalized by an ether-spacer-containing Gemini surfactant: Congo red adsorption and wettability. *Chemical Engineering Journal* **2018**, *349*, 388−396.

(7) Nafees, M.; Waseem, A. Organoclays as Sorbent Material for Phenolic Compounds: A Review. *Clean-Soil Air Water* **2014**, *42* (11), 1500−1508.

(8) Shen, T.; et al. Organo-vermiculites with biphenyl and dipyridyl gemini surfactants for adsorption of bisphenol A: Structure, mechanism and regeneration. *Chemosphere* **2018**, *207*, 489−496.

(9) Yu, M.; et al. Organo-vermiculites modified by low-dosage Gemini surfactants with different spacers for adsorption toward p-nitrophenol. *Colloids and Surfaces a-Physicochemical and Engineering Aspects* **2018**, *553*, 601−611.

(10) Wang, J.; et al. Insights into the efficient adsorption of rhodamine B on tunable organo-vermiculites. *Journal of Hazardous Materials* **2019**, *366*, 501−511.

(11) Shen, T.; et al. Efficient removal of mefenamic acid and ibuprofen on organo-Vts with a quinoline-containing gemini surfactant: Adsorption studies and model calculations. *Chemosphere* **2022**, *295*, No. 133846.

(12) Yang, S.; et al. The characterization of organo-montmorillonite modified with a novel aromatic-containing gemini surfactant and its comparative adsorption for 2-naphthol and phenol. *Chemical Engineering Journal* **2015**, *268*, 125−134.

(13) Karaman, C.; et al. Congo red dye removal from aqueous environment by cationic surfactant modified-biomass derived carbon: Equilibrium, kinetic, and thermodynamic modeling, and forecasting via artificial neural network approach. *Chemosphere* **2022**, *290*, No. 133346.

(14) Yu, M.; Gao, M.; Shen, T.; Zeng, H.; et al. Single and simultaneous adsorption of rhodamine B and congo red from aqueous solution by organo-vermiculites. *J. Mol. Liq.* **2019**, *292*, No. 111408.

(15) Shen, T.; et al. Single and simultaneous adsorption of basic dyes by novel organo-vermiculite: A combined experimental and theoretical study. *Colloids and Surfaces a-Physicochemical and Engineering Aspects* **2020**, *601*, No. 125059.

(16) Pi, Y.; et al. Vermiculite modified with alkylammonium salts: characterization and sorption of ibuprofen and paracetamol. *Chem. Pap.* **2021**, *75*, 4199−4216.

(17) Zang, W.; et al. Facile modification of homoionic-vermiculites by a gemini surfactant: Comparative adsorption exemplified by methyl orange. *Colloids Surf., A* **2017**, *533*, 99−108.

(18) Li, C.; et al. Mixtures of anionic surfactants with single/triple polyoxyethylene chains and Gemini quaternary ammonium surfactant: interaction and surface activity studies. *J. Mol. Liq.* **2021**, *343*, No. 117117, DOI: 10.1016/j.molliq.2021.117117.

(19) Liu, Y.; et al. Comparison between the removal of phenol and catechol by modified montmorillonite with two novel hydroxyl-containing Gemini surfactants. *Journal of Hazardous Materials* **2014**, *267*, 71−80.

(20) Park, Y.; Ayoko, G. A.; Frost, R. L. Application of organoclays for the adsorption of recalcitrant organic molecules from aqueous media. *J. Colloid Interface Sci.* **2011**, *354* (1), 292−305.

(21) Han, T.; et al. Enhanced corrosion inhibition of carbon steel by pyridyl gemini surfactants with different alkyl chains. *Mater. Chem. Phys.* **2020**, *240*, No. 122156.

(22) Bagherifam, S.; et al. Highly selective removal of nitrate and perchlorate by organoclay. *Appl. Clay Sci.* **2014**, *95*, 126−132.

(23) Taleb, K.; et al. Gemini surfactant modified clays: Effect of surfactant loading and spacer length. *Appl. Clay Sci.* **2018**, *161*, 48−56.

(24) Flores, F. M.; et al. Technological applications of organo-montmorillonites in the removal of Pyrimethanil from water: adsorption/desorption and flocculation studies. *Environmental Science and Pollution Research* **2017**, *24* (16), 14463−14476.

(25) Jaynes, W. F.; Boyd, S. A. Clay Mineral Type and Organic Compound Sorption by Hexadecyltrimethylammonium-exchanged Clays. *Soil Sci. Soc. Am. J.* **1991**, *55*, 43−48.

(26) Chen, B. L.; Zhu, L. Z.; Zhu, J. X. Configurations of the bentonite-sorbed myristylpyridinium cation and their influences on the uptake of organic compounds. *Environ. Sci. Technol.* **2005**, *39* (16), 6093−6100.

(27) Guo, S.; et al. Effective adsorption of sulfamethoxazole by novel Organo-Vts and their mechanistic insights. *Microporous Mesoporous Mater.* **2019**, *286*, 36−44.

(28) Ma, L.; et al. Adsorption of phenol and Cu(II) onto cationic and zwitterionic surfactant modified montmorillonite in single and binary systems. *Chemical Engineering Journal* **2016**, *283*, 880−888.

(29) Shen, T.; et al. Architecting organo silica nanosheets for regenerable cost-effective organics adsorbents. *Chemical Engineering Journal* **2018**, *331*, 211−220.

(30) Yu, X.; et al. Development of organovermiculite-based adsorbent for removing anionic dye from aqueous solution. *J. Hazard Mater.* **2010**, *180* (1−3), 499−507.

(31) Stawinski, W.; et al. Simultaneous removal of dyes and metal cations using an acid, acid-base and base modified vermiculite as a sustainable and recyclable adsorbent. *Sci. Total Environ.* **2017**, *576*, 398−408.

(32) Huang, P.; et al. Determining the Mechanism and Efficiency of Industrial Dye Adsorption through Facile Structural Control of Organo-montmorillonite Adsorbents. *ACS Appl. Mater. Interfaces* **2017**, *9* (31), 26383−26391.

(33) Janiak, C. A critical account on $\pi-\pi$ stacking in metal complexes with aromatic nitrogen-containing ligands †. *J. Chem. Soc., Dalton Trans.* **2000**, *21*, 3885−3896.

(34) Cao, G.; et al. Asymmetric gemini surfactants modified vermiculite- and silica nanosheets-based adsorbents for removing methyl orange and crystal violet. *Colloids and Surfaces a-Physicochemical and Engineering Aspects* **2020**, *596*, No. 124735.

(35) Rytwo, G.; Ruiz-Hitzky, E. Enthalpies of adsorption of methylene blue and crystal violet to montmorillonite - Enthalpies of adsorption of dyes to montmorillonite. *J. Therm. Anal. Calorim.* **2003**, *71* (3), 751−759.

(36) Dlugosz, O.; Banach, M. Kinetic, isotherm and thermodynamic investigations of the adsorption of Ag+ and Cu2+ on vermiculite. *J. Mol. Liq.* **2018**, *258*, 295−309.

(37) Liu, Y. Is the Free Energy Change of Adsorption Correctly Calculated? *J. Chem. Eng. Data* **2009**, *54* (7), 1981−1985.

(38) Kishor, R.; et al. Environment friendly degradation and detoxification of Congo red dye and textile industry wastewater by a newly isolated Bacillus cohnni (RKS9). *Environmental Technology & Innovation* **2021**, *22*, No. 101425.

https://doi.org/10.1021/acsomega.3c08363
ACS Omega 2024, 9, 4841−4848